Revision 1

Merwinite in diamond from São Luiz, Brazil: a new mineral of the Ca-rich mantle environment

Dmitriy A. Zedgenizov[1,2], Anton Shatskiy[1,2], Alexey L. Ragozin[1,2], Hiroyuki Kagi[3], Vladislav S. Shatsky[1,4]

[1]V.S. Sobolev Institute of Geology and Mineralogy, Russian Academy of Science, Siberian Branch, Koptyuga pr. 3, Novosibirsk 630090, Russia

[2]Novosibirsk State University, Novosibirsk 630090, Russia

[3]Geocheical Research Center, Graduate School of Science, University of Tokyo, Tokyo 113-0033, Japan

[4]A.P. Vinogradov Institute of Geochemistry, Russian Academy of Science, Siberian Branch, 1a Favorsky St., Irkutsk, 664033, Russia

Abstract

Diamonds from Juina province, Brazil and some others localities reveal the existence of a deep Ca-rich carbonate-silicate source different from ultramafic and eclogite compositions. In this study, we describe the first finding of merwinite ($Ca_{2.85}Mg_{0.96}Fe_{0.11}Si_{2.04}O_8$) in a diamond; it occurs as an inclusion in the central growth domain of a diamond from the São Luiz river alluvial deposits (Juina, Brazil). In addition, the diamond contains inclusions of walstromite-structured $CaSiO_3$ in the core and $(Mg_{0.86}Fe_{0.14})_2SiO_4$ olivine in the rim. According to available experimental data, under

mantle conditions, merwinite can only be formed in a specific Ca-rich and Mg- and Si-depleted enviroment that differs from any known mantle lithology (peridotitic or eclogitic). We suggest that such chemical conditions can occur during the interaction of subduction-derived calcium carbonatite melt with peridotitic mantle. The partial reduction of the melt could cause the simultaneous crystallization of Ca-rich silicates ($CaSiO_3$ and merwinite) and diamond at an early stage, and $(Mg_{0.86}Fe_{0.14})_2SiO_4$ olivine and diamond at a later stage, after the Ca-Mg exchange between carbonatite melt and peridotite has ceased. This scenario is supported by the presence of calcite microinclusions within merwinite.

Introduction

The São Luiz river alluvial deposits (Juina, Brazil) are a well-known source of sublithospheric diamonds as identified by their mineral inclusions (Harte et al. 1999; Hutchison et al. 2001; Kaminsky et al. 2001; Araujo et al. 2003; Hayman et al. 2005). The studies of mineral inclusions within diamonds from São Luiz and some others localities revealed the existence of a deep Ca-rich carbonate-silicate reservoir different from ultramafic and eclogite compositions, and the absence of several common mantle minerals, such as olivine, garnet and low-Ca pyroxene (Brenker et al. 2005). Following polyphase inclusions were reported: $CaSiO_3$+$CaSi_2O_5$±Ca_2SiO_4, $CaSiO_3$+$CaTiO_3$, $CaSiO_3$+$CaCO_3$, $CaMgSi_2O_6$+$CaCO_3$ (Joswig et al. 1999; Stachel et al. 2000; Kaminsky et al. 2001; Brenker et al. 2005, 2007; Hayman et al. 2005; Walter et al. 2008; Bulanova et al. 2010; Harte 2010; Zedgenizov et al. 2013). These inclusions suggest the presence of a chemically distinct reservoir in the sublithospheric convecting mantle. Several aspects,

47 e.g. the C-isotopic composition of the host diamonds (Bulanova et al. 2010; Walter et al.
48 2011; Zedgenizov et al. 2013) or Eu-anomalies of $CaSiO_3$ (Harte et al. 1999; Stachel et al.
49 2000, 2005), attributed the Ca-rich lithology to subduction processes. Additionally some
50 of the Ca-rich inclusions originate from the transition zone and even lower mantle
51 (Joswig et al. 1999; Kaminsky et al. 2001; Walter et al. 2008). In this study, we provide
52 the first report of a new Ca-rich inclusion in diamond, merwinite, from a diamond
53 discovered in the São Luiz river alluvial deposits.

54

55 **Methods**

56 The morphology of the diamond crystal was studied using a LEO 1430 VPSEM
57 scanning electron microscope (SEM). The diamond was subsequently polished to expose
58 its mineral inclusions. The polished plate was carbon-coated and put into a JEOL JXA-
59 8100 electron microprobe (EMP) at IGM SB RAS (Novosibirsk, Russia). The samples
60 were imaged in the electron backscattered (EBS) mode, and the inclusions were analysed
61 using a quantitative EMP analyzer at 15 kV accelerating voltage, 20 nA sample current
62 and 2 μm beam diameter. The internal uncertanty of each EMP analysis did not exceed
63 5%.

64 The internal structure of diamond was imaged using cathodoluminescence (CL)
65 coupled with SEM. The carbon isotope composition of the different diamond zones was
66 determined using a CAMECA IMS 1270 secondary ion mass spectrometer (SIMS) at the
67 University of Edinburgh (United Kingdom). The internal uncertanty of each carbon
68 isotopic analysis did not exceed 0.2 ‰. The internal structure of the diamond was
69 examined under cathodoluminescence (CL). Infrared absorption spectra of the studied

diamonds were recorded on an FTIR Bruker VERTEX 70 equipped with a HYPERION 2000 microscope. Local spectra with resolution of 4 cm^{-1} over the range the range 600–4500 cm^{-1}, were recorded by averaging 50 scans from an area of 50×50 μm. The contents of N-centres were calculated following a standard procedure (Mendelssohn and Milledge 1995). The intrinsic absorption of diamonds (12.3 cm^{-1} at 2030 cm^{-1}) was taken to be the internal standard (Zaitsev 2001). The decomposition of the spectrum from 1100 to 1350 cm^{-1} made it possible to determine the contribution of different N-defects with characteristic absorptions of specified shapes.

Results

The diamond (~1.7mm in size) is a colorless, with rounded tetrahexahedroid morphology (Fig. 1a,b), whereas its internal structure, as visualized by the CL images, reveals octahedral growth zones (Fig. 1c). The CL images reveals a dark diamonds core and a brighter rim (Fig. 1c,d). The brighter rim shows parallel lines intersecting the octahedral growth zones (Fig. 1c,d). Generally this feature is considered as a sign of plastic deformation (Lang 1977) which is very common in Juina diamonds (Hutchison et al. 1999).

The two growth domains differ in N content: the core is N-free (type IIa) while the rim contains 20–25 ppm of N with a low aggregation state (21–30 % IaB). In addition, an absorption band at 3107 cm^{-1} is evident in the infrared absorption spectrum of the N-bearing rim. This band is related to a carbon-hydrogen bond stretching mode (Woods and Collins 1983).

Four individual inclusions were exposed in different growth zones. Two inclusions of $CaSiO_3$ and a single inclusion of $Ca_{2.85}Mg_{0.96}Fe_{0.11}Si_{2.04}O_8$ are located in the central growth domain (Fig. 1c,d). A single inclusion of $(Mg_{0.86}Fe_{0.14})_2SiO_4$ was observed in the outer growth domain (Fig. 1c). The size of the inclusions varies from 5 to 12 μm. The inclusions compositions are given in Table 1. The Raman spectra of the inclusions were consistent with those of walstromite (Brenker et al. 2007), merwinite (Piriou and McMillan 1983) and olivine (Chopelas 1991) (Fig. 2). The Raman spectrum of merwinite contains additional peaks assignable to calcite (Fig. 2b). Although specimen was heated to 300-400 °C during polishing, the Raman spectra of mineral inclusions show no evidence of amorphization, which can be expected for high-pressure phases such as Mg-Si-perovskite.

The studied diamond has a relatively heavy carbon isotope composition $\delta^{13}C$ = -1.8 to -3.4 ‰, in comparison with the average mantle $\delta^{13}C$ ~ -5 ‰ (Harte 2010); and the $\delta^{13}C$ valeus show no correlation to the growth zones.

Discussion

It was pointed out that the heavier $\delta^{13}C$ values correspond well with those of marine carbonate sediments (Stachel et al. 2005; Tappert et al. 2005). Harte (2010) also argued that the formation of many superdeep diamonds was probably triggered by the dehydration of deeply subducted material. Walter et al. (2008) have provided experimental and geochemical evidence that Ca-silicate mineral inclusions in some diamonds from Juina, Brazil, crystallized from primary and evolved carbonate melts in the mantle transition zone. They suggest a process whereby subducted carbonated

115 oceanic crust undergoes low-degree partial melting to produce carbonate melts.
116 Metasedimentary carbon in altered oceanic crust consists of a mixture of organic
117 components ($\delta^{13}C \approx -27‰$) and marine carbonates ($\delta^{13}C \approx 0‰$) (Shilobreeva et al. 2011).

118 The internal texture of the studied diamond exhibits a primary octahedral growth
119 morphology (Fig. 1c); this is reminiscent of diamonds grown from hydrous carbonatite
120 melt upon gradual reduction by hydrogen fluids in experiments at 6 GPa (Pal'yanov et al.
121 2002). The external shape of the studied crystal exhibits a rounded dissolution
122 morphology, similar to the rounded tetrahexahedroid. This habit suggests that the original
123 octahedron lost about 50 % of its initial weight as a result of dissolution in the water-
124 bearing $CaCO_3$ or kimberlite melt (Khokhryakov and Pal'yanov 2007, 2010). The $CaSiO_3$
125 inclusions found in the same growth zone with merwinite inclusion can be interpreted as
126 former Ca-Si perovskite, i.e. mineral of the transition zone or lower mantle (Harte 2010).
127 Yet, under mantle conditions, merwinite is unusual and can be only formed in specific
128 Ca-rich and Mg- and Si-depleted environments (Yoder 1968; Sharp et al. 1986;
129 Moriyama et al. 1992; Safonov et al. 2007; Luth 2009), which differs from any known
130 mantle lithology (peridotitic, eclogitic or pelitic). Such chemical conditions can be
131 achieved during interaction of subduction-derived calcio-carbonatite melt with peridotitic
132 mantle. Carbonatite melts are very mobile and rapidly infiltrate peridotite wall-rock by
133 dissolution-precipitation mechanism (Hammouda and Laporte 2000) because the dihedral
134 angle at the contacts between silicate minerals and melt is lower than 60º (Hunter and
135 McKenzie 1989; Minarik and Watson 1995) and because the diffusivity of silicate solute
136 in the carbonatite melt is high (Shatskiy et al. 2013b). According to the experimental
137 studies of Hammouda (2003) and Grassi and Schmidt (2011), partial melting of the

uppermost part of the subducted slab (i.e., carbonated eclogite and pelite) yields a $CaCO_3$-rich carbonatite melt. This melt differs from the magnesio-dolomitic carbonatite melt that can coexist with the peridotitic mantle (Dasgupta and Hirschmann 2007; Brey et al. 2008). Therefore, subduction-derived calcio-carbonatite melt must react with overlying host mantle to form Ca-bearing silicates and a Ca-dolomite carbonatite melt. The following reactions between alkali-bearing $CaCO_3$ melt and peridotite were experimentally established at 6.5 GPa (Sharygin et al. 2012):

$$4Mg_2Si_2O_6\ (OPx) + 8CaCO_3\ (Liq) = Mg_2SiO_4\ (Ol) + CaMgSi_2O_6\ (CPx) + Ca_3MgSi_2O_8\ (Mw) + 3SiO_2\ (Liq) + 4CaMg(CO_3)_2\ (Liq); \quad (1)$$

$$2Mg_2SiO_4\ (Ol) + 6CaCO_3\ (Liq) = Ca_3MgSi_2O_8\ (Mw) + 3CaMg(CO_3)_2\ (Liq); \quad (2)$$

In short (< 6 h) experiments, merwinite was found at the melt-olivine interface at 1400 °C and at the melt-orthopyroxene interface at 1300 °C. However, once the infiltrated melt approaches an equilibrium (Ca-dolomitic) composition during re-equilibration with peridotite mantle, merwinite crystallization terminates and CPx replaces merwinite. At higher temperatures, the merwinite-forming reactions do not occur and the interaction of $CaCO_3$ melt with the OPx + Ol assemblage yields direct formation of the CPx + Ol assemblage (Sharygin et al. 2012). That is, the finding of a merwinite inclusion in diamond is consistent with the above experimental evidence, and indicates its crystallization from a $CaCO_3$-rich carbonatite melt infiltrated into peridotite mantle.

Diamond formation requires a continuous carbon supply to the growing crystals, i.e., supersaturation of the solution with carbon (e.g. as with a carbonatite melt; Pal'yanov et al. 1999a). It requires continuous reduction of carbonatite melt (Pal'yanov et al. 2002), which should inevitably occur during its interaction with reduced surrounding mantle

(Frost and McCammon 2008). The partial reduction of $CaCO_3$-rich, SiO_2-bearing melt should cause precipitation of silicate solutes simultaneously with a diamond crystallization. Therefore, at the early stage the diamond entraps the Ca-rich silicates: $CaSiO_3$ (walstromite or perovskite) and $Ca_3MgSi_2O_8$ (merwinite), as we found in the central growth domain of this specimen. This scenario is supported by the presence of calcite as microinclusions within the merwinite inclusion, as is evident from the Raman spectra (Fig. 2b). At a later stage, the carbonatite melt becomes a Ca-dolomitic in composition due to Ca-Mg exchange with peridotitic mantle. The reduction of this melt could also cause precipitation of $(Mg_{0.86}Fe_{0.14})_2SiO_4$, which has been found as an inclusion in the outer growth domain. The relatively high Fe-content in this inclusion may suggest an Fe enrichment of the parental carbonatite melt. Indeed, subduction-derived carbonatite melts formed as a result of partial melting of carbonated eclogite or pelite are Fe-rich (Hammouda 2003; Grassi and Schmidt 2011).

Alternatively, the carbonatite melt can be partially reduced, and continuous carbon supply could occur via carbonate-silicate reactions, which proceed slightly below the CCO ($C + O_2 = CO_2$) oxygen buffer (Ogasawara et al. 1997; Palyanov et al. 2005). One of these reactions, previously suggested by Luth (1993), has been experimentally established at 6.5 GPa and 1400 °C in a long-duration experiment (16 h) (Sharygin et al. 2012):

$$3Mg_2Si_2O_6\ (OPx) + 2CaCO_3\ (Liq) = 2Mg_2SiO_4\ (Ol) + 2CaMgSi_2O_6\ (CPx) + 2C + 2O_2. \quad (3)$$

Based on the available experimental data on the merwinite-forming carbonate-silicate reactions (Sharygin et al. 2012), kinetics of diamond crystallization in the

carbonatite melt (Pal'yanov et al. 1999b, 2002), and melting phase relations in the carbonate and carbonate-silicate systems (Hammouda 2003; Grassi and Schmidt 2011; Litasov et al. 2013; Shatskiy et al. 2013a, 2013c, 2013d), the most probable growth conditions of the studied diamond are 1150-1400 °C and pressures exceeding 6 GPa. According to the phase relations in the CaO-SiO_2 system, the $CaSiO_3$ compounds can stabilize as walstromite in the pressure range of 4-10 GPa, and as perovskite above 12-14 GPa (Huang and Wyllie 1975; Gasparik et al. 1994; Akaogi et al. 2004). Merwinite has been found to be a stable phase at least up to 16 GPa and 2000 °C (Moriyama et al. 1992). Thus, we can conclude that the inner growth zone of the studied diamond could form either under the upper mantle conditions (6 GPa < P < 10 GPa) or in the transition zone (14 < $P \leq$ 16 GPa). Dependently from the upper pressure limit of the mervinite stability field (which is unknown) this pressure range can be extended to the lower mantle. The outer olivine-hosting zone could crystallize at a later time at the same or shallower depth in the upper mantle.

The presence of merwinite in the studied diamond from the São Luiz suggests a process whereby subduction-derived Ca-carbonatite melt reacts with host peridotitic mantle to form Ca-rich silicates ($CaSiO_3$ and merwinite) and cause diamond formation. Under mantle conditions, merwinite can only be formed in a specific Ca-rich and Mg- and Si-depleted enviroment that differs from any known mantle lithology (peridotitic or eclogitic). Thus, merwinite could be an apparent evidence of Ca-carbonatite metasomatism in the deep mantle.

Acknowledgements

We are grateful to Ofra Klein-BenDavid, Mark Hutchison and two anonymous reviewers for thorough reviews and useful suggestions and Ian Swainson for editorial handling, telling criticism and comments. This work was supported by the Ministry of education and science of Russian Federation (project Nos. 14.B37.21.0601 and 14.B25.31.0032), by the Russian Foundation for Basic Research (project Nos. 12-05-33035 and 13-05-00628) and Integration Project of SB RAS (project No. IP16).

Table 1. Composition (EMP-analysis) of inclusions in diamond 88 from São Luiz river alluvial deposits.

	Walstromite		Merwinite		Olivine	
	wt%	mol%	wt%	mol%	wt%	mol%
SiO_2	51.6	50.3	36.8	34.2	39.8	33.4
TiO_2	0.04	0.03	0.02	0.01	0.0	0.0
Al_2O_3	0.01	0.01	0.10	0.05	0.0	0.0
Cr_2O_3	0.0	0.0	0.02	0.01	0.09	0.03
FeO	0.31	0.26	2.32	1.80	13.6	9.62
MnO	0.00	0.00	0.04	0.03	0.04	0.03
MgO	0.00	0.00	11.7	16.1	45.4	56.8
CaO	47.3	49.4	47.9	47.6	0.12	0.10
Na_2O	0.03	0.03	0.24	0.22	0.0	0.0
K_2O	0.00	0.00	0.01	0.00	0.0	0.0
NiO	n.d.	n.d.	n.d.	n.d.	0.25	0.17
Total	99.3	100.0	99.1	100.0	99.3	100.0

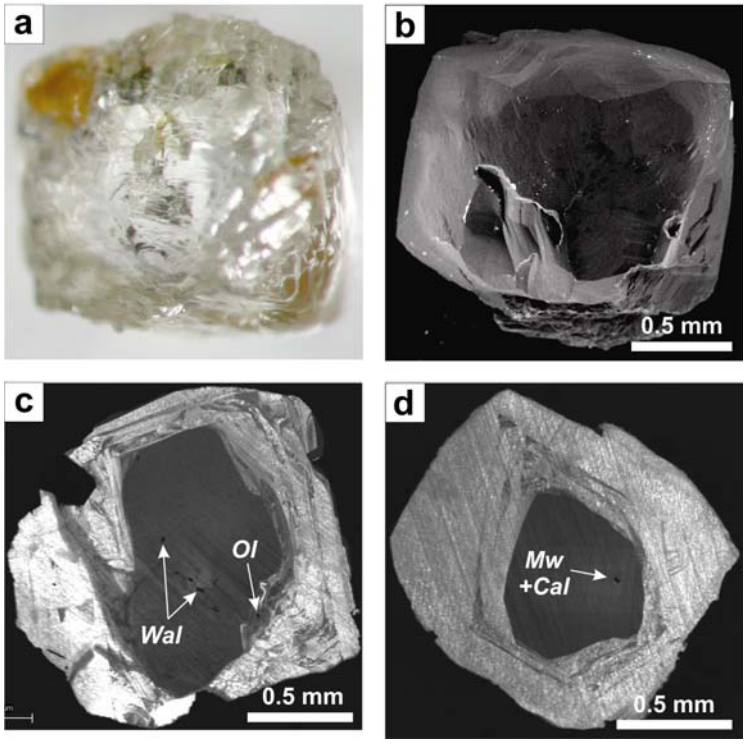

Fig. 1. The external and internal morphology of diamond no. 88 from São Luiz river alluvial deposits. (a) Optical photomicrograph and (b) BSE image of the diamond before polishing. (c, d) Cathodoluminescence images of both sides of a (110) diamond plate (~300 μm in thickness) mounted into epoxy (black). Wal = $CaSiO_3$ walstromite,

Mw+Cal = $Ca_{2.85}Mg_{0.96}Fe_{0.11}Si_{2.04}O_8$ merwinite inclusion containing calcite, Ol = $(Mg_{0.86}Fe_{0.14})_2SiO_4$ olivine.

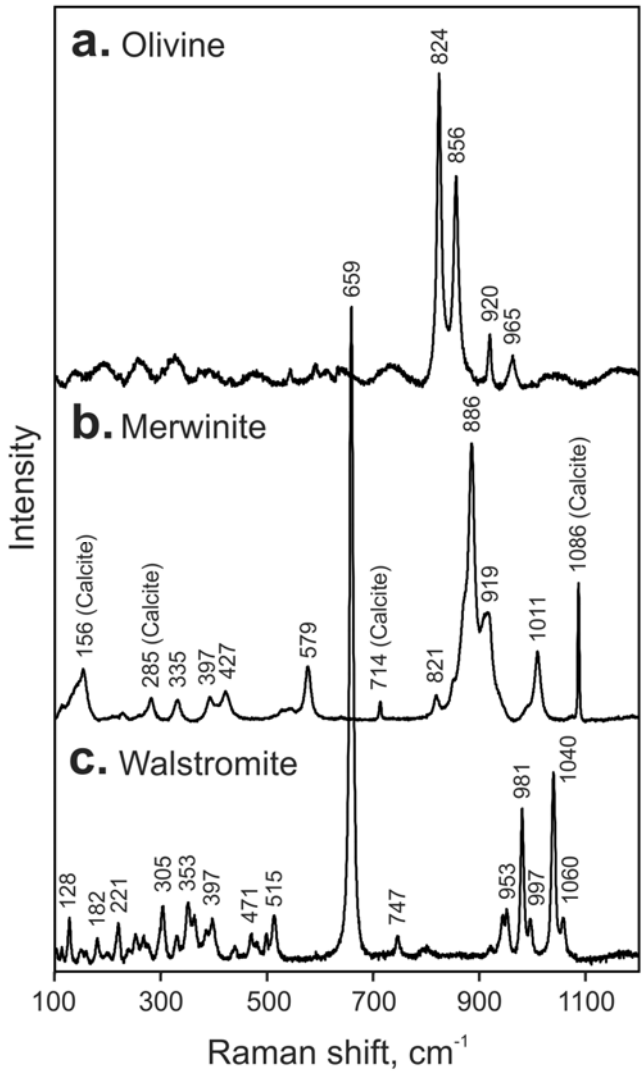

Fig. 2. Raman spectra of mineral inclusions in diamond no. 88 from São Luiz river alluvial deposits: $(Mg_{0.86}Fe_{0.14})_2SiO_4$ olivine (a), $Ca_{2.85}Mg_{0.96}Fe_{0.11}Si_{2.04}O_8$ merwinite and calcite (b) and $CaSiO_3$ walstromite (c).

References

Akaogi, M., Yano, M., Tejima, Y., Iijima, M., and Kojitani, H. (2004) High-pressure transitions of diopside and wollastonite: phase equilibria and thermochemistry of $CaMgSi_2O_6$, $CaSiO_3$ and $CaSi_2O_5$-$CaTiSiO_5$ system. Physics of the Earth and Planetary Interiors, 143, 145-156.

Araujo, D.P., Gaspar, J.C., Yingwei, F., Hauri, E.H., Hemley, R., and Bulanova, G.P. (2003) Mineralogy of diamonds from the Juina province, Brazil. VIIIth International Kimberlite Conference, Victoria, Canada.

Brenker, F.E., Vincze, L., Vekemans, B., Nasdala, L., Stachel, T., Vollmer, C., Kersten, M., Somogyi, A., Adams, F., Joswig, W., and Harris, J.W. (2005) Detection of a Ca-rich lithology in the Earth's deep (> 300 km) convecting mantle. Earth and Planetary Science Letters, 236, 579-587.

Brenker, F.E., Vollmer, C., Vincze, L., Vekemans, B., Szymanski, A., Janssens, K., Szaloki, I., Nasdala, L., Joswig, W., and Kaminsky, F. (2007) Carbonates from the lower part of transition zone or even the lower mantle. Earth and Planetary Science Letters, 260, 1-9.

Brey, G.P., Bulatov, V.K., Girnis, A.V., and Lahaye, Y. (2008) Experimental melting of carbonated peridotite at 610 GPa. Journal of Petrology, 49, 797-821.

Bulanova, G.P., Walter, M.J., Smith, C.B., Kohn, S.C., Armstrong, L.S., Blundy, J., and Gobbo, L. (2010) Mineral inclusions in sublithospheric diamonds from Collier 4 kimberlite pipe, Juina, Brazil: subducted protoliths, carbonated melts and primary kimberlite magmatism. Contributions to Mineralogy and Petrology, 160, 489-510.

Chopelas, A. (1991) Single crystal Raman spectra of forsterite, fayalite, and monticellite. American Mineralogist, 76, 1101-1109.

Dasgupta, R., and Hirschmann, M.M. (2007) Effect of variable carbonate concentration on the solidus of mantle peridotite. American Mineralogist, 92, 370-379.

Frost, D.J., and McCammon, C.A. (2008) The redox state of Earth's mantle. Annual Review of Earth and Planetary Sciences, 36, 389-420.

Gasparik, T., Wolf, K., and Smith, C.M. (1994) Experimental determination of phase relations in the $CaSiO_3$ system from 8 to 15 GPa. American Mineralogist, 79, 1219-1222.

Grassi, D., and Schmidt, M.W. (2011) The melting of carbonated pelites from 70 to 700 km depth. Journal of Petrology, 52, 765-789.

Hammouda, T. (2003) High-pressure melting of carbonated eclogite and experimental constraints on carbon recycling and storage in the mantle. Earth and Planetary Science Letters, 214, 357-368.

Hammouda, T., and Laporte, D. (2000) Ultrafast mantle impregnation by carbonatite melts. Geology, 28, 283-285.

Harte, B. (2010) Diamond formation in the deep mantle: the record of mineral inclusions and their distribution in relation to mantle dehydration zones. Mineralogical Magazine, 74, 189-215.

Harte, B., Harris, J.W., Hutchison, M.T., Watt, G.R., and Wilding, M.C. (1999) Lower mantle mineral associations in diamonds from São Luiz, Brazil. In Y. Fei, C.M. Bertka, and B.O. Mysen, Eds. Mantle Petrology: Field Observations and High Pressure Experimentation; a tribute to Francis R. (Joe) Boyd, 6, p. 125-153. The Geochemical Society Special Publication

Hayman, P.C., Kopylova, M.G., and Kaminsky, F.V. (2005) Lower mantle diamonds from Rio Soriso (Juina area, Mato Grosso, Brazil). Contributions to Mineralogy and Petrology, 149, 430-445.

Huang, W.L., and Wyllie, P.J. (1975) Melting and subsolidus phase relationships for $CaSiO_3$ to 35 kilobars pressure. American Mineralogist, 60(3-4), 213-217.

Hunter, R.H., and McKenzie, D. (1989) The equilibrium geometry of carbonate melts in rocks of mantle composition. Earth and Planetary Science Letters, 92, 347-356.

Hutchison, M.T., Hursthouse, M.B., and Light, M.E. (2001) Mineral inclusions in diamonds: associations and chemical distinctions around the 670-km discontinuity. Contributions to Mineralogy and Petrology, 142, 119-126.

Hutchison, M.T., Cartigny, P., and Harris, J.W. (1999) Carbon and nitrogen compositions and physical characteristics of transition zone and lower mantle diamonds from Sao Luiz, Brazil. In J.J. Gurney, Ed. VIIth International Kimberlite Conference, I, p. 372-382. Red Roof Design, Cape Town.

Joswig, W., Stachel, T., Harris, J.W., Baur, W.H., and Brey, G.P. (1999) New Ca-silicate inclusions in diamonds - tracers from the lower mantle. Earth and Planetary Science Letters, 173, 1-6.

Kaminsky, F.V., Zakharchenko, O.D., Davies, R., Griffin, W.L., Khachatryan-Blinova, G.K., and Shiryaev, A.A. (2001) Superdeep diamonds from the Juina area, Mato Grosso State, Brazil. Contributions to Mineralogy and Petrology, 140(6), 734-753.

Khokhryakov, A.F., and Pal'yanov, Y.N. (2007) The evolution of diamond morphology in the process of dissolution: Experimental data. American Mineralogist, 92, 909-917.

Khokhryakov, A.F., and Pal'yanov, Y.N. (2010) Influence of the fluid composition on diamond dissolution forms in carbonate melts. American Mineralogist, 95, 1508-1514.

Lang, A. (1977) Defects in natural diamonds: recent observations by new methods. Journal of Crystal Growth, 42, 625-631.

Litasov, K.D., Shatskiy, A., Ohtani, E., and Yaxley, G.M. (2013) The solidus of alkaline carbonatite in the deep mantle. Geology, 41, 79-82.

Luth, R.W. (1993) Diamonds, eclogites, and the oxidation state of the Earth's mantle. Science, 261, 66-68.

Luth, R.W. (2009) The activity of silica in kimberlites, revisited. Contributions to Mineralogy and Petrology, 158, 283-294.

Mendelssohn, M., and Milledge, H. (1995) Geologically significant information from routine analysis of the mid-infrared spectra of diamonds. International Geology Review, 37, 95-110.

Minarik, W.G., and Watson, E.B. (1995) Interconnectivity of carbonate melt at low melt fraction. Earth and Planetary Science Letters, 133, 423-437.

Moriyama, J., Kawabe, I., Fujino, K., and Ohtani, E. (1992) Experimental study of element partitioning between majorite, olivine, merwinite, diopside and silicate melts at 16 GPa and 2,000 ^{o}C. Geochemical Journal, 26, 357-382.

Ogasawara, Y., Liou, J.G., and Zhang, R.Y. (1997) Thermochemical calculation of log fO_2–T–P stability relations of diamond-bearing assemblages in the model system CaO–MgO–SiO_2–CO_2–H_2O. Russian Geology and Geophysics, 546-557.

Pal'yanov, Y.N., Sokol, A.G., Borzdov, Y.M., Khokhryakov, A.F., Shatsky, A.F., and Sobolev, N.V. (1999a) The diamond growth from Li_2CO_3, Na_2CO_3, K_2CO_3 and Cs_2CO_3 solvent-catalysts at P=7 GPa and T=1700-1750 ^{o}C. Diamond and Related Materials, 8, 1118-1124.

Pal'yanov, Y.N., Sokol, A.G., Borzdov, Y.M., Khokhryakov, A.F., and Sobolev, N.V. (1999b) Diamond formation from mantle carbonate fluids. Nature, 400, 417-418.

Pal'yanov, Y.N., Sokol, A.G., Borzdov, Y.M., Khokhryakov, A.F., and Sobolev, N.V. (2002) Diamond formation through carbonate-silicate interaction. American Mineralogist, 87, 1009-1013.

Palyanov, Y.N., Sokol, A.G., Tomilenko, A.A., and Sobolev, N.V. (2005) Conditions of diamond formation through carbonate-silicate interaction. European Journal of Mineralogy, 17, 207-214.

Piriou, B., and McMillan, P. (1983) The high-frequency vibrational spectra of vitreous and crystalline orthosilicates. American Mineralogist, 68, 426-443.

Safonov, O.G., Perchuk, L.L., and Litvin, Y.A. (2007) Melting relations in the chloride-carbonate-silicate systems at high-pressure and the model for formation of alkalic diamond-forming liquids in the upper mantle. Earth and Planetary Science Letters, 253, 112-128.

Sharp, Z.D., Essene, E.J., Anovitz, L.M., Metz, G.W., Westrum, E.F., Hemingway, B.S., and Valley, J.W. (1986) The heat-capacity of a natural monticellite and phase-equilibria in the system CaO-MgO-SiO_2-CO_2. Geochimica et Cosmochimica Acta, 50, 1475-1484.

Sharygin, I.S., Litasov, K.D., Shatskiy, A., Safonov, O.G., Ohtani, E., and Pokhilenko, N.P. (2012) Interaction of orthopyroxene with carbonatite melts at 3 and 6.5 GPa: Implication for evolution of kimberlite magma. G-COE Symposium 2012 "Achievement of G-COE Program for Earth and Planetary Science", p. 146-149, Sendai, Japan.

Shatskiy, A., Gavryushkin, P.N., Sharygin, I.S., Litasov, K.D., Kupriyanov, I.N., Higo, Y., Borzdov, Y.M., Funakoshi, K., Palyanov, Y.N., and Ohtani, E. (2013a) Melting and subsolidus phase relations in the system Na_2CO_3-$MgCO_3$+-H_2O at 6 GPa and the stability of $Na_2Mg(CO_3)_2$ in the upper mantle. American Mineralogist, DOI: http://dx.doi.org/10.2138/am.2013.4418.

Shatskiy, A., Litasov, K.D., Borzdov, Y.M., Katsura, T., Yamazaki, D., and Ohtani, E. (2013b) Silicate diffusion in alkali-carbonatite and hydrous melts at 16.5 and 24 GPa: Implication for the melt transport by dissolution-precipitation in the transition zone and uppermost lower mantle. Physics of the Earth and Planetary Interiors, http://dx.doi.org/10.1016/j.pepi.2013.09.004.

Shatskiy, A., Sharygin, I.S., Gavryushkin, P.N., Litasov, K.D., Borzdov, Y.M., Shcherbakova, A.V., Higo, Y., Funakoshi, K., Palyanov, Y.N., and Ohtani, E.

(2013c) The system K_2CO_3-$MgCO_3$ at 6 GPa and 900-1450 ºC. American Mineralogist, 98, 1593-1603.

Shatskiy, A., Sharygin, I.S., Litasov, K.D., Borzdov, Y.M., Palyanov, Y.N., and Ohtani, E. (2013d) New experimental data on phase relations for the system Na_2CO_3-$CaCO_3$ at 6 GPa and 900-1400 ºC. American Mineralogist, DOI: http://dx.doi.org/10.2138/am.2013.4436.

Shilobreeva, S., Martinez, I., Busigny, V., Agrinier, P., and Laverne, C. (2011) Insights into C and H storage in the altered oceanic crust: Results from ODP/IODP Hole 1256D. Geochimica et Cosmochimica Acta, 75, 2237-2255.

Stachel, T., Brey, G.P., and Harris, J.W. (2005) Inclusions in Sublithospheric Diamonds: Glimpses of Deep Earth. Elements, 1(73 – 78).

Stachel, T., Harris, J.W., Brey, G.P., and Joswig, W. (2000) Kankan diamonds (Guinea) II: lower mantle inclusion parageneses. Contributions to Mineralogy and Petrology, 140, 16-27.

Tappert, R., Stachel, T., Harris, J.W., Muehlenbachs, K., Ludwig, T., and Brey, G.P. (2005) Diamonds from Jagersfontein (South Africa): messengers from the sublithospheric mantle. Contributions to Mineralogy and Petrology, 150, 505-522.

Walter, M.J., Bulanova, G.P., Armstrong, L.S., Keshav, S., Blundy, J.D., Gudfinnsson, G., Lord, O.T., Lennie, A.R., Clark, S.M., Smith, C.B., and Gobbo, L. (2008) Primary carbonatite melt from deeply subducted oceanic crust. Nature, 454, 622-630.

Walter, M.J., Kohn, S.C., Araujo, D., Bulanova, G.P., Smith, C.B., Gaillou, E., Wang, J., Steele, A., and Shirey, S.B. (2011) Deep Mantle Cycling of Oceanic Crust: Evidence from Diamonds and Their Mineral Inclusions. Sciencexpress.

Woods, G.S., and Collins, A.T. (1983) Infrared absorption spectra of hydrogen complexes in type I diamonds. Journal of Physics and Chemistry of Solids, 44, 471-475.

Yoder, H.S. (1968) Akermanite and related melilite-bearing assemblages. Carnegie Institute Washington Yearbook, 66, 471-477.

Zaitsev, A.M. (2001) Optical properties of diamond: a data handbook. 502 p. Springer-Verlag, Berlin.

Zedgenizov, D.A., Kagi, H., Shatsky, V.S., and Ragozin, A.L. (2013) Local variations of carbon isotope composition in diamonds from São Luiz (Brazil): evidence for heterogenous carbon reservoir in sublithospheric mantle. Chemical Geology, DOI: 10.1016/j.chemgeo.2013.10.033.